NASA Technical Paper 1091

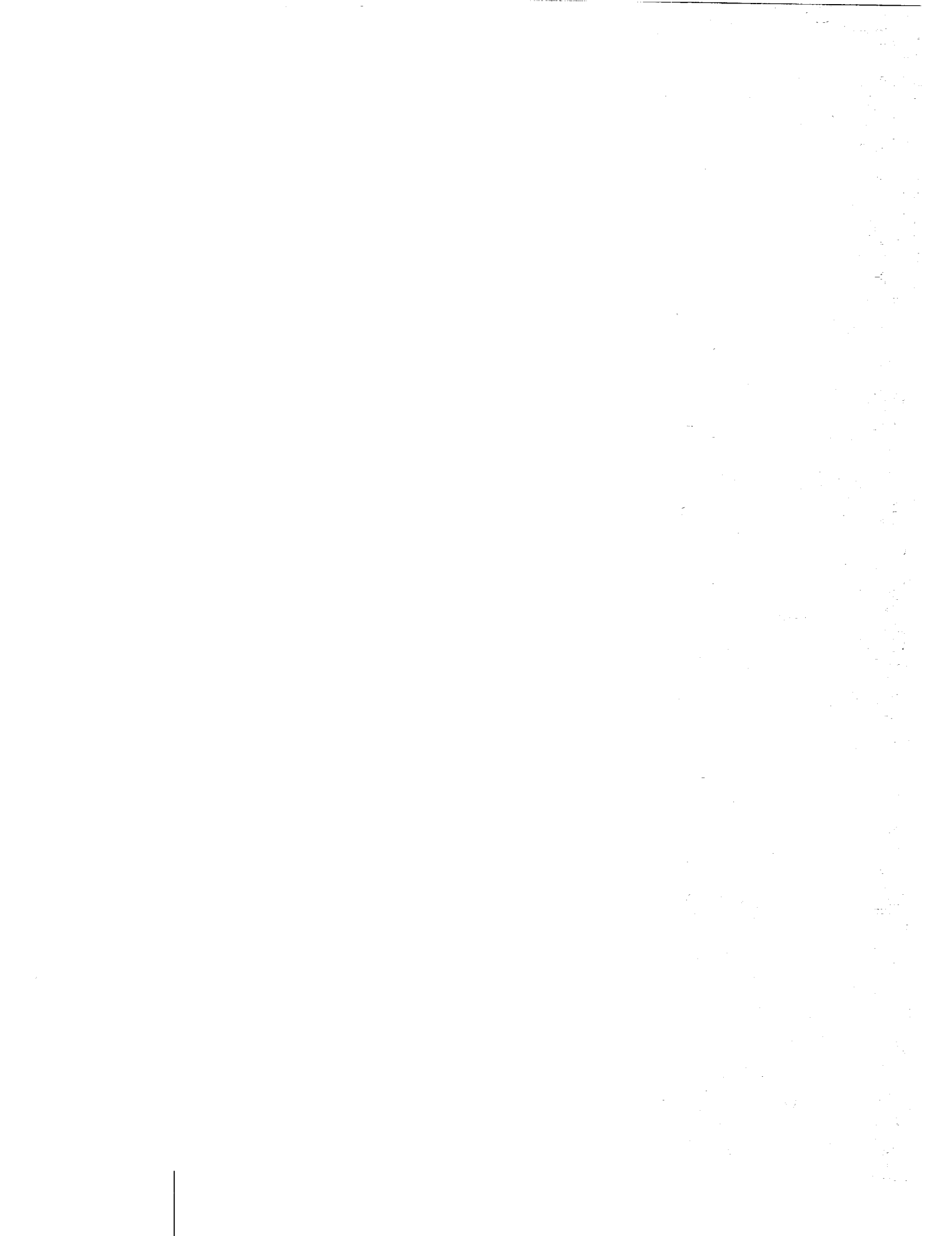# Experimental Performance of a 13.65-Centimeter-Tip-Diameter Tandem-Bladed Sweptback Centrifugal Compressor Designed for a Pressure Ratio of 6

CASE FILE COPY

Hugh A. Klassen, Jerry R. Wood,
and Lawrence F. Schumann

NOVEMBER 1977

NASA

Experimental Performance of a 13.65-Centimeter-Tip-Diameter Tandem-Bladed Sweptback Centrifugal Compressor Designed for a Pressure Ratio of 6

Hugh A. Klassen
Lewis Research Center
Cleveland, Ohio

Jerry R. Wood and Lawrence F. Schumann
Propulsion Laboratory
U.S. Army R&T Laboratories (AVRADCOM)
Cleveland, Ohio

EXPERIMENTAL PERFORMANCE OF A 13.65-CENTIMETER-TIP-DIAMETER
TANDEM-BLADED SWEPTBACK CENTRIFUGAL COMPRESSOR
DESIGNED FOR A PRESSURE RATIO OF 6

by Hugh A. Klassen, Jerry R. Wood, and Lawrence F. Schumann

Lewis Research Center and
U. S. Army Air Mobility R&D Laboratory

SUMMARY

A 13.65-centimeter-tip-diameter backswept centrifugal compressor with a tandem inducer was experimentally investigated to determine if there was any performance improvement over more conventional compressors in the same mass flow and pressure ratio range. The compressor was designed for a total pressure ratio of 6.19:1 at an equivalent mass flow rate of 0.907 kilogram per second and an equivalent speed of 80 000 rpm. Overall stage performance with a two row cascade vane diffuser was determined for four impeller exit to shroud axial clearances. Impeller characteristics with a vaneless diffuser were also obtained for four values of design speed axial tip clearances.

At design equivalent speed and an impeller axial tip clearance of 7.6 percent of exit blade height, peak overall total efficiency was 0.765 at a pressure ratio of 5.90. At design equivalent speed, flow range between choke and surge decreased from 12.5 to 6.3 percent of choking flow as axial tip clearance was decreased from 20.7 to 7.6 percent. Design equivalent mass flow rate at design speed was 0.44 percent below the inducer choking flow rate. This indicated an area deficiency in the inducer. With the cascade diffuser, stage choking is controlled by the diffuser for operation below 92 percent equivalent speed for 7.6 percent clearance.

For the tests with the vaneless diffuser, peak impeller efficiency at design speed increased from 0.767 to 0.813, and peak pressure ratio increased as axial tip clearance was decreased from 20.7 to 8.4 percent. At an equivalent mass flow rate of 0.785 kilogram per second, the impeller pressure ratio increased from 5.88 to 6.43 and the work factor increased slightly from 0.773 to 0.783.

Design impeller exit axial tip clearance was 2.7 percent. Because of impeller deflection at surge, the lowest clearance tested was nearly three times larger than the design value. Data taken with the four clearance settings were extrapolated to obtain stage performance at design clearance. Extrapolated stage pressure ratio and efficiency were 6.1 and 0.783, respectively. The extrapolated static pressure distribution along the shroud of the impeller and diffuser indicated a lower than design static pressure at the impeller exit. The static pressure rise through the diffusing system was very close to design intent.

INTRODUCTION

In recent years, there has been a renewed interest in the use of centrifugal compressors in gas turbine engines for small engine applications such as helicopters, auxiliary power units (APU), general aviation, surface vehicles, etc., as well as for the last stage of large core engines. This interest results from initial cost savings, ruggedness, and high single-stage pressure ratios attainable with centrifugal compressors. As a result of this interest, the Lewis Research Center has initiated a program to investigate single-stage centrifugal compressors designed for pressure ratios between 6 and 10 and equivalent mass flow rates of approximately 1 kilogram per second. The program is intended to establish baseline performance for current single-stage compressors and to evaluate advanced concepts that have the potential to improve stage efficiency and surge to choke flow range. Concepts such as tandem inducer and diffuser blading, boundary layer bleed, vortex generators, variable area diffusers, and partial admission may be considered.

As part of this program, an advanced technology compressor with a tandem-bladed backswept impeller and two-row cascade vane diffuser was experimentally evaluated. The design mass flow rate is 0.907 kilogram per second and the design overall pressure ratio is 6.19:1. Design equivalent speed is 80 000 rpm. A tandem-bladed impeller design was selected in order to utilize transonic axial compressor technology in the inducer design. The function of the axial inducer is to reduce the supersonic velocity at the tip to subsonic with minimum loss. A second advantage of a separate inducer is that the inducer boundary layer is dumped at the trailing edge and a fresh boundary layer is started at the leading edge of the centrifugal impeller. The cascade diffuser was selected to minimize boundary layer losses. Fresh boundary layers start at the leading edge of the second blade row.

The purpose of testing this compressor was to determine if the tandem inducer and cascade diffuser produce a significant improvement in compressor performance as compared to more conventional compressors. Overall compressor performance and impeller performance with a vaneless diffuser in place of the cascade vane diffuser were obtained. The vaneless diffuser test was also used to determine if there were any impeller-diffuser matching problems. Tests were made at four design speed axial tip clearances to establish the effect of axial clearance on impeller performance for 6:1 pressure ratio backswept designs.

This report presents the performance characteristics obtained for this 6:1 pressure ratio backswept centrifugal compressor. Overall performance is shown with curves of efficiency and total pressure ratio as functions of equivalent mass flow, equivalent speed, and axial tip clearance. Impeller performance with a vaneless diffuser is shown as curves of efficiency and total pressure ratio as functions of equivalent mass flow and

2

axial tip clearance at design speed. In addition, design velocity diagrams, design impeller loading diagrams, and static pressure profiles are presented.

SYMBOLS

$\Delta h'$ specific work, J/kg

N rotative speed, rpm

N_s specific speed, dimensionless

p pressure, N/m^2

Q volume flow rate, m^3/sec

T temperature, K

U blade speed, m/sec

V absolute gas velocity, m/sec

W relative gas velocity, m/sec

w mass flow rate, kg/sec

α absolute flow angle, deg from meridional plane

β relative flow angle, deg from meridional plane

γ ratio of specific heats

Δ change in clearance, percent of blade height at exit

δ ratio of inlet total pressure to U.S. standard sea level pressure, p'/p^*

η compressor adiabatic temperature rise efficiency, (ideal total enthalpy rise)/(actual total enthalpy rise)

θ ratio of compressor inlet total temperature to U.S. standard sea-level temperature, T'/T^*

ω impeller angular velocity, rad/sec

$\bar{\omega}$ diffuser total pressure loss coefficient, $(p_3' - p_4')/(p_3' - p_3)$

Ω mass flow-speed parameter, $\left[(w/N)/(w/N)_{design}\right]^*$

Subscripts:

cr   condition corresponding to Mach number of 1

id   ideal

m   meridional component

3

max   maximum value

min   minimum value

u   tangential component

0   station at bellmouth inlet

1   inducer inlet (fig. 8)

2   inducer exit - impeller inlet (fig. 8)

3   impeller exit (fig. 8)

4   exit of vaneless space downstream from cascade diffuser (fig. 8)

Superscripts:

'   absolute total state

*   U. S. standard sea-level conditions (temperature, 288.15 K; pressure, 10.13 N/cm^2 abs)

COMPRESSOR AERODYNAMIC DESIGN

The tandem impeller consists of a separate inducer followed by a centrifugal impeller. The inducer was designed by standard transonic axial compressor methods. Its function is to reduce the relative velocity at the tip from supersonic at the inlet to subsonic at the exit with minimum losses. The inducer is separated from the centrifugal impeller by an axial gap of 0.254 centimeter. Figure 1 shows a photograph of the tandem impeller. Figure 2 shows a meridional profile of the inducer/impeller and diffuser. Figures 3 and 4 show design velocity diagrams for the inducer and impeller, respectively. Figure 5 shows impeller design loading diagrams. Table I gives design details of the inducer and impeller. Impeller efficiency and pressure ratio are calculated outside the blade row assuming no aerodynamic blockage and constant specific heat (γ = 1.395). Additional design information is contained in reference 1.

Impeller exit flow is reduced from supersonic to subsonic in a constant area (decreasing axial width) vaneless space before entering the two row cascade vane diffuser having 22 vanes per row. Figure 6 shows the shapes and arrangement of the diffuser blades as well as the diffuser design velocity triangles. A second vaneless space downstream from the diffuser provides additional velocity reduction. Table II gives design details of the diffuser and vaneless spaces. Reference 1 gives additional design information. References 2 and 3 contain analytical studies of the relationship between tandem stator geometry and performance.

For the vaneless diffuser tests, a constant area vaneless space identical to the one used in the cascade diffuser test was blended into a constant axial width (0.401 cm)

4

passage at a radius 1.2 times the impeller exit radius (same location as vane leading edge in cascade diffuser tests). The flow exited from the constant axial width passage into a sudden expansion which had an axial width of 0.762 centimeter at a radius 1.29 times the impeller exit radius.

The overall design operating characteristics are as follows:

Equivalent mass flow rate, $w\sqrt{\theta}/\delta$, kg/sec 0.907

Total pressure ratio, p_4'/p_0' 6.19

Equivalent speed, $N/\sqrt{\theta}$, rpm 80 000

Specific speed, $N_s = \omega\sqrt{Q}/(h_{id}')^{3/4}$ 0.769

Total efficiency, η_{0-4} 0.817

APPARATUS, INSTRUMENTATION, AND PROCEDURE

Test Facility

Figure 7 shows a schematic of the compressor test facility. The compressor and turbine are on a common shaft. Compressor mass flow rate was measured with a choked flow nozzle on the inlet line and with the calibrated bellmouth on the compressor inlet. Compressor inlet pressure was automatically controlled by a valve on the inlet line to the plenum chamber. Compressor discharge pressure was manually controlled with a remotely operated valve in the compressor discharge line. Drive turbine speed was automatically controlled by a valve on the turbine inlet line. A hydrogen combustor was used to provide turbine inlet temperatures up to approximately 480 K. Turbine discharge pressure was manually controlled by two remotely operated valves in the turbine discharge line.

Instrumentation

The compressor instrument stations are shown in figure 8. The compressor inlet instrumentation is located in the plenum chamber and consists of two combination total temperature - total pressure probes spaced 90° apart. Each probe measures four total pressure samples and two total temperature samples. The bellmouth was instrumented with three static taps located in the throat. The discharge measuring station (station 4) is located in the second vaneless space downstream of the diffuser vanes (fig. 1) where the design Mach number is 0.203. This station consists of three total pressure probes and three shielded total temperature probes. Static pressures were measured along the impeller shroud and along the diffuser to the discharge measuring station. At the

impeller exit (station 3), static pressure was obtained from the average of five static taps spanning 1.5 diffuser vane pitches. For the impeller performance tests with the vaneless diffuser, static pressures were measured along the shroud and in the vaneless space. Instrumentation at stations 3 and 4 was the same as for the cascade diffuser tests.

Procedure

All tests were run with air at an inlet total temperature of approximately 292 K. Inlet total pressure was approximately 9.9 newtons per square centimeter. At design speed, overall compressor performance was obtained at design speed axial tip clearance values of 7.6, 12.5, 16.8, and 20.7 percent of exit blade height. For the vaneless tests the clearance was 8.4, 11.4, 16.3, and 20.7 percent. Clearance was varied by shimming the shroud away from the impeller. The diffuser position was not changed so that vaneless space passage height increased as the clearance increased. At each design speed clearance setting, data were also obtained at 50, 60, 70, 80, and 90 percent of design equivalent speed. The change in percent clearance with speed as determined by rub probes is shown in figure 9. The base point of zero at 100 percent speed was chosen so that the percent clearance at any speed can be determined by adding any value on the curve to the design speed percent clearance value. Mass flow rate was varied from choke to surge. The compressor work used to compute overall efficiency was obtained from the real gas enthalpy increase across the impeller. Total enthalpies at the compressor inlet and exit were obtained from the measured total temperatures at stations 0 and 4 using tables of real gas properties.

Impeller total efficiencies and pressure ratios were calculated from measured total temperatures accounting for variable specific heat and assuming no aerodynamic blockage at the impeller exit, since only trends were desired. The exit blade speed U was obtained from the measured rotative speed. The exit tangential velocity V_u was obtained from the relation $UV_u = \Delta h'$. The remainder of the velocity diagram was constructed from continuity using the measured equivalent mass flow, the static pressure at impeller exit, and no aerodynamic blockage. The resulting calculated total pressure was used to calculate impeller efficiency and pressure ratio. In order to obtain absolute values of impeller efficiency and pressure ratio, detailed knowledge of actual flow conditions at the impeller exit would be required.

6

RESULTS AND DISCUSSION

The test results are presented in three sections. In the first section, overall compressor performance is shown over a range of equivalent speeds. In the second section, impeller characteristics are shown for design equivalent speed. For these tests, the cascade vane diffuser was replaced by a vaneless diffuser. This allowed testing the impeller over its entire operating range and eliminated recirculation losses associated with circumferential pressure gradients. In the third section, impeller-diffuser matching characteristics are shown over a range of equivalent speeds.

Overall Compressor Performance

Design speed compressor performance with a vaned diffuser was obtained at design speed axial tip clearance values of 7.6, 12.5, 16.8, and 20.7 percent of impeller exit blade height. For each design speed clearance setting, performance was also obtained over a range of equivalent speed from 50 to 90 percent of design in increments of 10 percent without any change in shim size.

Overall compressor efficiency is presented in figure 10 and shows the strong influence of impeller exit to shroud axial tip clearance on efficiency at all speeds. Peak efficiency increased with speed to a value of 0.765 very near surge at 100 percent speed for the 7.6 percent design speed axial tip clearance setting. The data points identified with "S" were obtained close to surge.

Figure 11 shows the peak overall efficiency from figure 10 plotted against actual axial tip clearance. The actual clearance for each speed was obtained from figure 9. All the data can be represented by a quadratic which indicates a peak efficiency of about 79 percent if zero axial tip clearance were possible.

Figure 12 shows the effect of axial tip clearance on pressure ratio. There is very little change in total pressure ratio with clearance below 70 percent speed. The peak pressure ratio of 5.9 occurs near stage surge at 100 percent speed for the 7.6 percent clearance setting. At 70, 80, and 90 percent speeds the surge flow increases slightly as clearance is decreased. At 100 percent speed this increase is quite pronounced. Choking mass flow at 100 percent speed remained constant at 0.911 kilogram per second (0.44 percent above design flow) for all clearances indicating that the inducer is controlling the stage choke. Flow range as a percent of choking flow decreased from 12.5 percent at 20.7 percent clearance to 6.3 percent at 7.6 percent clearance for the 100 percent speed line. At 90 percent speed and below, stage choking flow increases as clearances are decreased. This is a result of diffuser controlled choke at 90 percent speed

and below and an increase in total pressure ratio across the impeller as clearance is decreased.

Impeller Performance Obtained With Vaneless Diffuser

To determine impeller performance, the original cascade vane diffuser was replaced by a vaneless diffuser. Tests were made at design speed axial tip clearances corresponding to 8.4, 11.4, 16.3, and 20.7 percent of blade height. All results presented in this section are for design speed.

Figure 13 shows impeller total efficiency as a function of equivalent mass flow and axial tip clearance. As stated in the Procedure section, the impeller efficiency was calculated assuming no aerodynamic blockage at the impeller exit. Impeller efficiencies calculated with 10 percent aerodynamic blockage at the impeller exit were about 1.5 points higher than they were when calculated with no aerodynamic blockage assumed. The compressor was surged only with the 16.3 percent clearance. Figure 14 shows peak impeller efficiency for the vaneless tests and for the cascade diffuser tests. The data show no measurable difference in peak impeller efficiency obtained with the vaneless and cascade diffuser tests. This indicates that recirculation losses associated with this particular configuration are negligible. These losses perhaps do not occur on this configuration because of the reduction of vaneless space axial width used to achieve a constant area vaneless space between impeller exit and cascade diffuser entry (fig. 2(a)). The reduction in axial width resulting from sloping the shroud sidewall acts to decrease the stream tube thickness near the shroud and reduce the amount of diffusion of the meridional component of velocity near the shroud. This would tend to produce a more uniform meridional velocity profile and reduce the tendency of the shroud wall boundary layer to separate and flow back into the impeller. Since the tangential velocity profile should be rather uniform, the resultant flow angle distribution at the diffuser vanes would be more uniform and the incidence variation along the diffuser blade span would be less than that for a comparable parallel wall diffuser.

The circumferential static pressure gradient at the impeller exit for design speed had a maximum variation of 4 to 5 percent for the cascade diffuser test whereas for the vaneless diffuser test it was only about 2 percent. This small difference in circumferential pressure gradient between the two tests could also contribute to the lack of indicated recirculation loss.

Impeller peak efficiency increased 4.6 points from 0.767 to 0.813 as the clearance was reduced from 20.7 to 8.4 percent. A quadratic curve fit indicates an impeller efficiency of 0.854 could be obtained if zero axial tip clearance were possible. Figure 15 shows that at a given flow rate pressure ratio increased with decreasing clearance. At an equivalent mass flow rate of 0.785 kilogram per second the pressure ratio increased

8

from 5.88 to 6.43. At this flow rate, the pressure ratio is close to maximum. Surge of the system was recorded at only one value of axial tip clearance (16.3 percent) and indicated a flow range of 17.3 percent of choking flow.

Figure 16 shows work factor as a function of equivalent mass flow and axial tip clearance. At a given flow rate the work factor increased slightly with decreasing clearance. At an equivalent flow rate of 0.785 kilogram per second the work factor increased from 0.773 to 0.783 or about 1.3 percent as the clearance was decreased from 20.7 to 8.4 percent. This is probably due to the increased amount of air that flows through the clearance gap as clearance is increased. This fluid is not being worked on by the impeller as much as the flow that is going through the impeller channels; thus, its work factor will be less than that of the main through flow. Resultant mixing at the impeller exit will produce an average work factor that is dependent on the amount of clearance. Thus, increasing the clearance could yield smaller work factors.

Impeller-Diffuser Matching Characteristics

Figure 17 shows impeller efficiency and diffuser total pressure loss coefficient $\bar{\omega}$ for 70 percent speed and above for a design speed clearance setting of 7.6 percent. At 70 percent speed, there is a large mismatch between the diffuser and impeller since peak impeller efficiency and minimum diffuser total pressure loss coefficient occur at greatly different mass flows (0.370 kg/sec for minimum $\bar{\omega}_{3-4}$ and 0.510 kg/sec for peak η_{0-3}). The match becomes progressively better as speed increases. At 100 percent speed, minimum $\bar{\omega}_{3-4}$ occurs at a mass flow of 0.855 kilogram per second while peak η_{0-3} occurs at a mass flow of 0.885 kilogram per second.

The points brought out in the previous discussion are graphically summarized in figure 18. In this figure the mass flow parameter Ω for stage choke, stage surge, peak impeller efficiency, minimum diffuser total pressure loss, and minimum flow with the vaneless diffuser (near or at surge) are plotted against percent equivalent speed. In reference 4 it was shown that when stage choking flow is plotted in this manner a positive slope indicates inducer choke. For this compressor an inflection in the stage choke curve occurred at about 92 percent speed. This indicates that the diffuser and inducer are choking at the same mass flow at this speed. Below 92 percent speed the diffuser is causing stage choke and above 92 percent speed the inducer is causing stage choke.

The variations of mass flow for peak impeller efficiency and minimum diffuser total pressure loss $\bar{\omega}_{3-4}$ are shown as two bands in figure 18. The peak efficiency band represents the difference in mass flow that corresponds to peak efficiency minus 0.001. The impeller efficiency is approximately a constant value of 0.813 in this band. The minimum $\bar{\omega}_{3-4}$ band represents the difference in mass flow that corresponds to minimum $\bar{\omega}_{3-4}$ plus 0.01. The total pressure loss coefficient varies from 0.10 to 0.11 in this

9

band. Both bands are observed to intersect at design speed. This indicates that from the standpoint of peak stage efficiency the components are well matched. Stage surge, however, occurs at approximately the same mass flow. Since the minimum mass flow with the vaneless diffuser is considerably less than the stage surge mass flow, at all speeds, it is evident that the vaned diffuser is causing stage surge. If stage surge is being caused by a positive incidence angle on the diffuser blades, than a rotation of the diffuser vanes toward tangential will reduce the incidence angle for a given mass flow. The mass flow will then be lower at the stalling incidence. The rotation of the diffuser vanes toward tangential will also reduce the diffuser throat area and thus move the minimum $\bar{\omega}_{3-4}$ of the diffuser toward lower mass flows and thus match at a lower impeller efficiency (fig. 13). However, since the impeller efficiency from the vaneless diffuser test is relatively flat with changes in mass flow it is possible the penalty for moving the minimum $\bar{\omega}_{3-4}$ of the diffuser to lower mass flows will be small. A decrease in the diffuser throat area by about 10 percent appears to be needed to reduce the stage surge mass flow to approximately the minimum mass flow observed for the vaneless diffuser test. If the stage performance decreases significantly with a simple rotation of the diffuser vanes toward tangential, a removal of one or more blades accompanied with a respacing of the remaining vanes may achieve the desired change in incidence angle with little or no change in throat area and thus keep the characteristics of each component matched for peak efficiency.

COMPARISON TO DESIGN

In table I the design exit axial tip clearance at 100 percent speed is 0.0126 centimeter or 2.7 percent of the exit blade. The closest clearance that was investigated was 0.0353 centimeter or 7.6 percent with the cascade diffuser. The clearance value shown in figure 9 was taken at a flow point away from surge. During surge at the 7.6 percent clearance setting, the rub probes at the impeller exit indicated near zero clearance. Since the smallest clearance tested is much greater than the design value, direct comparison did not seem reasonable. Redesign of the impeller disk would probably allow closer clearances to be tested. Figures 19 and 20 show extrapolations of performance with the cascade diffuser at design clearance based on the four clearances tested. The surge line in figure 12 was used to project a surge flow of 0.878 kilogram per second at design clearance. The extrapolations from figure 19 indicate that pressure ratio at design clearance and the extrapolated surge mass flow would be about 6.1, which is slightly lower than the design value of 6.19. Overall efficiency would be about 0.783 or 3.4 points lower than the design value of 0.817. Impeller efficiency at design clearance from figure 14 is 0.84, which is 5 points lower than design.

10

Figure 20 represents a comparison of (1) the design static pressure rise through the stage, (2) the best static pressure rise obtained with the cascade and vaneless diffuser tests, and (3) the extrapolated static pressure rise at design clearance. The extrapolated values at impeller exit fall somewhat short of design intent. This decrement in static pressure persists through the diffuser to the discharge measuring station and indicates that the stage performance was below the design value because of poor performance in the impeller as mentioned earlier.

SUMMARY OF RESULTS

The performance of a 13.65-centimeter-tip-diameter centrifugal compressor with a tandem inducer and cascade diffuser was investigated. After obtaining overall performance data at four values of design speed axial tip clearance, the cascade diffuser was replaced with a vaneless diffuser to determine impeller performance over a range of axial tip clearances similar to those for the vaned tests.

The following results were obtained from overall stage performance tests:

1. Peak overall efficiency at design aerodynamic speed and 7.6 percent axial tip clearance was 0.765. Peak total pressure ratio was 5.9. The design axial tip clearance of 2.7 percent could not be obtained with the configuration tested. However, extrapolations of data obtained at the four clearances tested to the design clearance yielded a design speed peak efficiency of 0.783 compared to the design value of 0.817 and a design speed peak total pressure ratio of 6.1 compared to the design value of 6.19.

2. Flow range at design speed based on a percentage of choking mass flow decreased from 12.5 to 6.3 percent as the axial tip clearance was reduced from 20.7 to 7.6 percent.

3. Equivalent choking mass flow at design speed was 0.911 kilogram per second, which is 0.44 percent greater than the design equivalent mass flow of 0.907 kilogram per second.

4. For the 7.6 percent design speed axial tip clearance setting, at equivalent speeds less than 92 percent, choking mass flow is governed by the diffuser, while at speeds greater than 92 percent, choking mass flow is governed by the inducer.

The following results were obtained for design equivalent speed from impeller tests with the cascade diffuser replaced with a vaneless diffuser:

1. Peak impeller efficiency at design speed increased from 0.767 to 0.813 as the axial tip clearance was reduced from 20.7 to 8.4 percent. Extrapolation of the data obtained at the four clearances tested to the design clearance yielded a design speed peak impeller efficiency of 0.84 compared to the design value of 0.89.

2. Peak impeller pressure ratio increased from 5.88 to 6.43 as the clearance was reduced from 20.7 to 8.4 percent.

11

3. At an equivalent mass flow rate of 0.785 kilogram per second, the work factor increased from 0.773 to 0.783 as clearance was reduced from 20.7 to 8.4 percent.

4. Recirculation losses for the cascade diffuser tests were negligible since the calculated impeller efficiencies for the vaned test were approximately the same as those for the vaneless test.

5. The flow range of the system at 16.3 percent clearance was 17.3 percent of choking mass flow rate.

Lewis Research Center,
    National Aeronautics and Space Administration,
        and
U.S. Army Air Mobility R&D Laboratory,
    Cleveland, Ohio, July 28, 1977,
        505-04.

REFERENCES

1. Bryce, C. A.; et al.: Small, High Pressure Ratio Compressor:Aerodynamic and Mechanical Design. (APS-5404-R-Vol-1, AiResearch Mfg, Co.; NAS 3-14306.) NASA CR-120941, 1973.

2. Sanger, Nelson L.: Analytical Study of the Effects of Geometric Changes on the Flow Characteristics of Tandem-Bladed Compressor Stators. NASA TN D-6264, 1971.

3. Sanger, Nelson L.: Analytical Study on a Two-Dimensional Plane of the Off-Design Flow Properties of Tandem-Bladed Compressor Stators. NASA TM X-2734, 1973.

4. Klassen, Hugh A.; Wood, Jerry R.; and Schumann, Lawrence F.: Experimental Performance of a 16.10-Centimeter-Tip-Diameter Sweptback Centrifugal Compressor Designed for a 6:1 Pressure Ratio. NASA TM X-3552, 1977.

TABLE I. - INDUCER AND IMPELLER

DESIGN SUMMARY

Characteristic	Inducer	Impeller
Number of blades	24	24
Inlet tip diameter, cm	9.27	9.27
Inlet hub/tip ratio	0.5	0.65
Exit blade angle, deg	-----	30.8
Exit tip diameter, cm	9.27	13.65
Impeller exit blade height, cm	-----	0.467
Design axial tip clearance at impeller exit/exit blade height	-----	0.027
Total pressure ratio:		
p_2'/p_0'	1.525	-----
p_3'/p_2'	-----	4.515
p_3'/p_0'	-----	6.885
Total efficiency:		
η_{0-2}	0.943	-----
η_{2-3}	-----	0.887
η_{0-3}	-----	.890

TABLE II. - DIFFUSER DESIGN SUMMARY

Characteristic	Vaneless space 1	Cascade vane diffuser	Vaneless space 2
Radius ratio, exit/inlet	1.2	1.375	1.42
Inlet Mach number	1.099	0.853	0.306
Exit Mach number	0.853	0.306	0.203
Compressor total pressure ratio at exit	6.58:1	6.25:1	6.19:1
Compressor total efficiency at exit	0.853	0.823	0.817
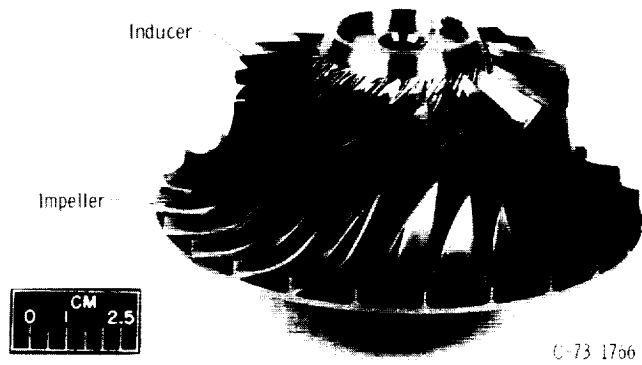
Figure 1. - Tandem impeller.
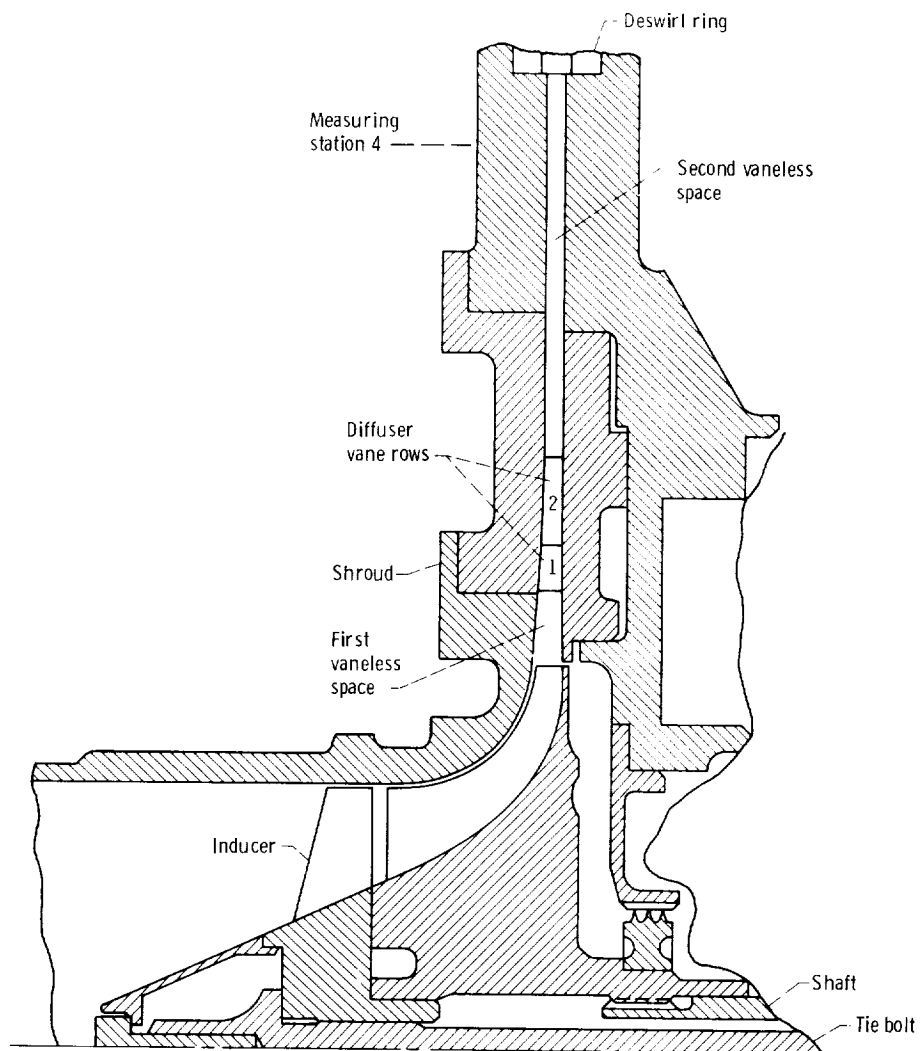
(a) Aerodynamic component assembly.

Figure 2. - Meridional view of compressor.

14
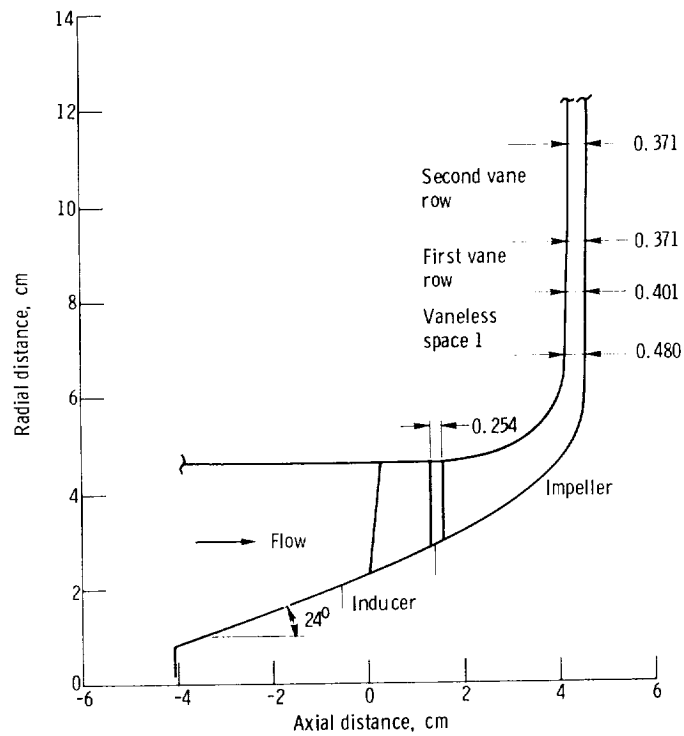
(b) Meridional flow path.

Figure 2. – Concluded.

Inlet

$\dfrac{U}{V_{cr}} = 1.01$; $V_{cr} = 310.6$ m/sec

1.16; $V_{cr} = 334.1$ m/sec

$\dfrac{U}{V_{cr}} = 0.997$; $V_{cr} = 330.1$ m/sec

0.739; $V_{cr} = 328.3$ m/sec
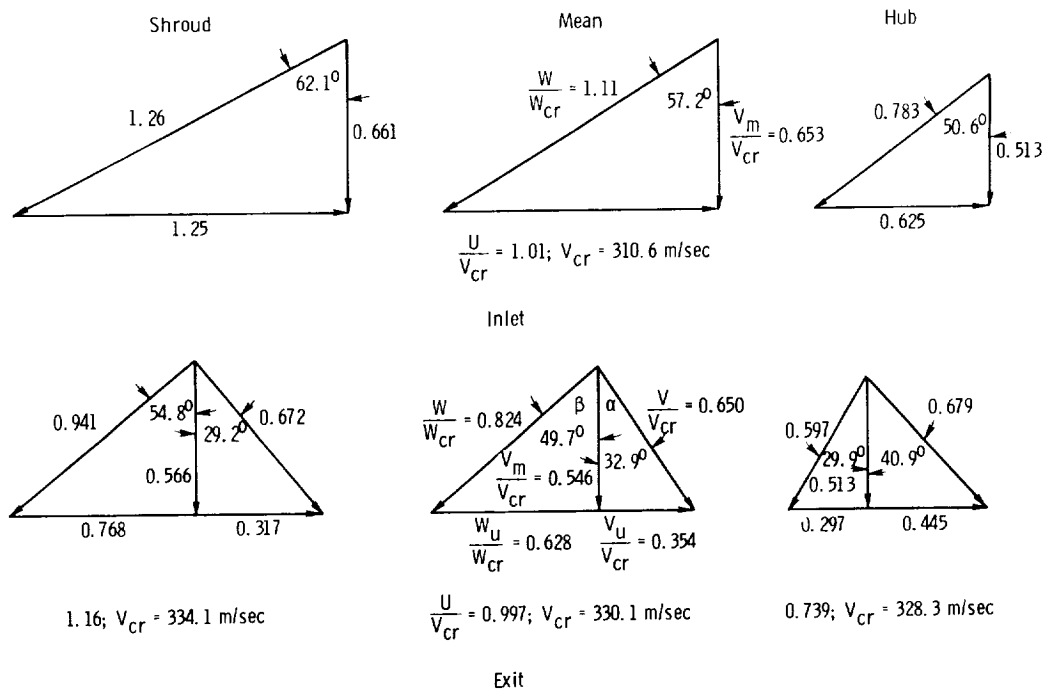
Exit

Figure 3. – Inducer design velocity diagrams for inside blade.

15
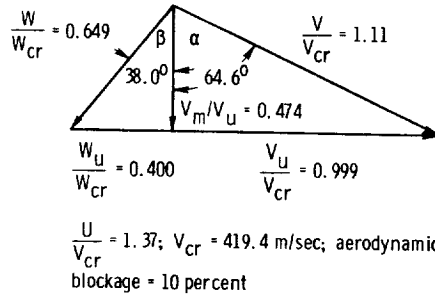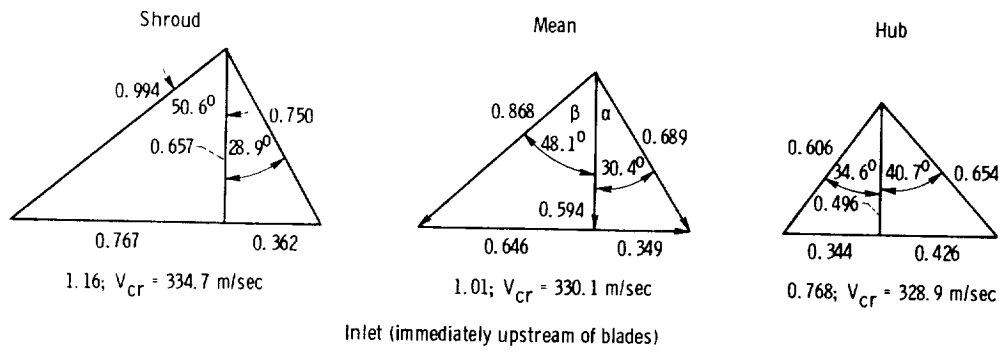
Figure 4. - Impeller design velocity diagrams.

(a) At shroud.

(b) At hub.
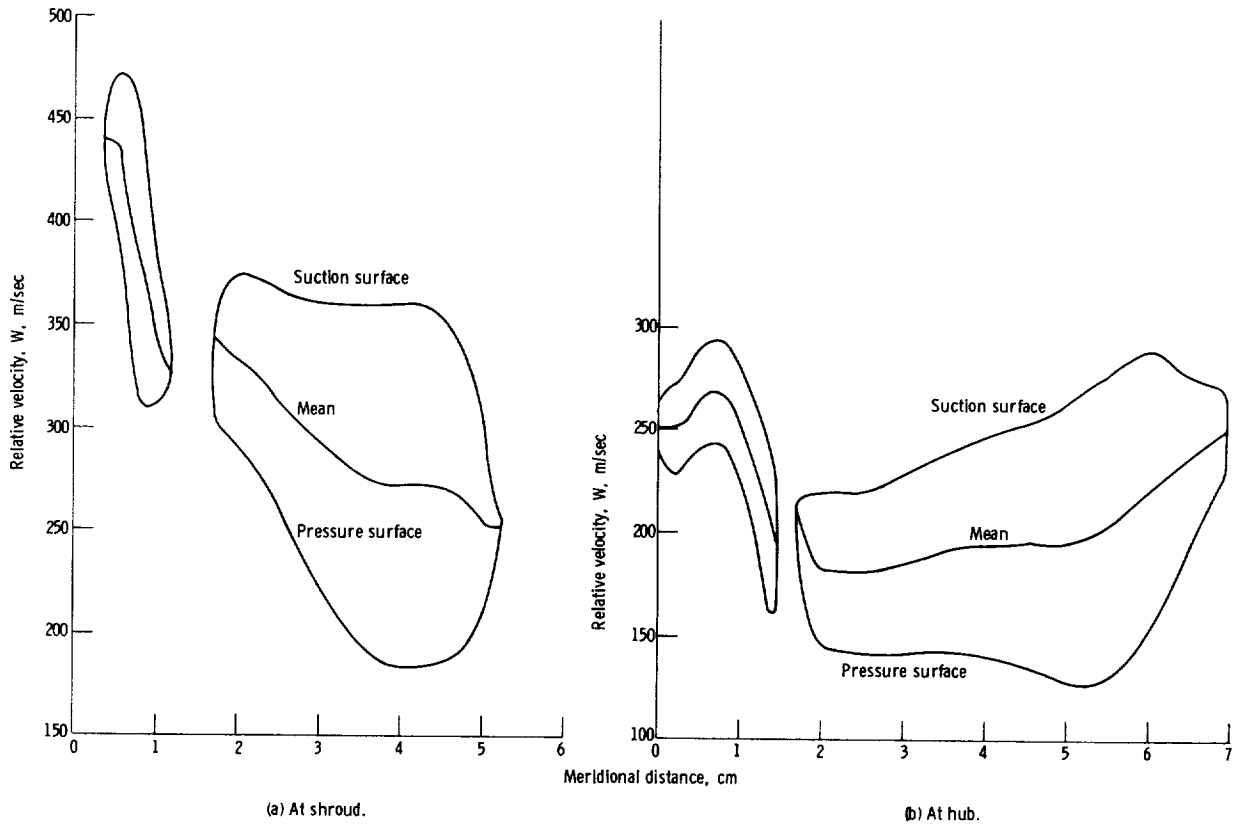
Figure 5. - Impeller design loading diagram.

16
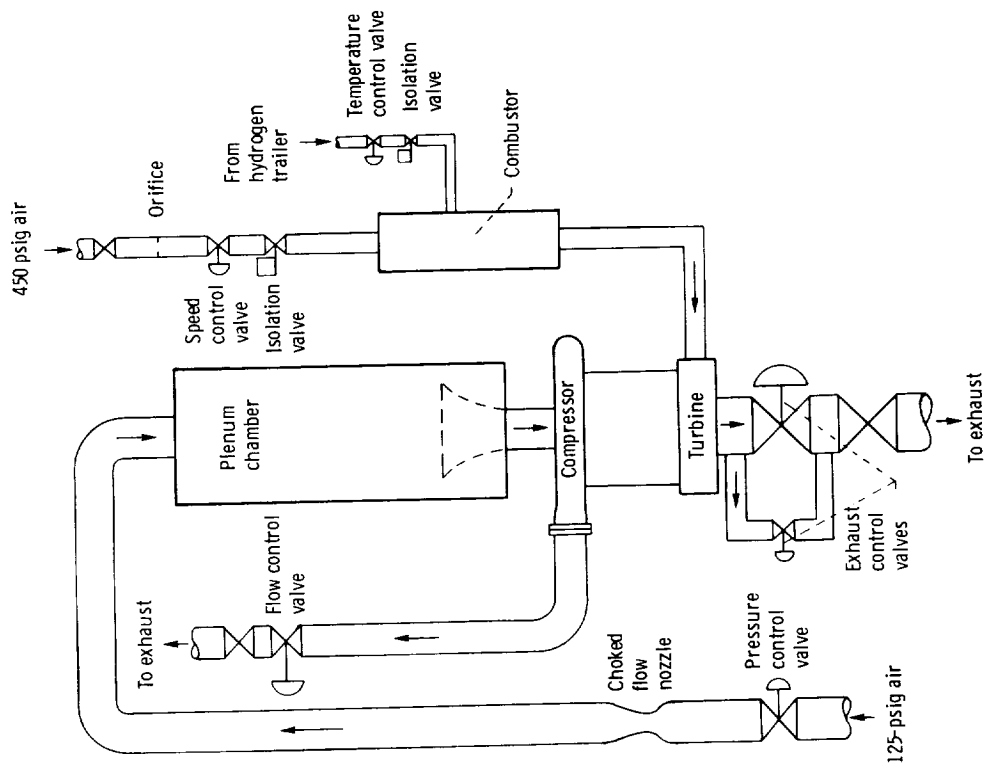
Figure 7. - Test facility schematic.
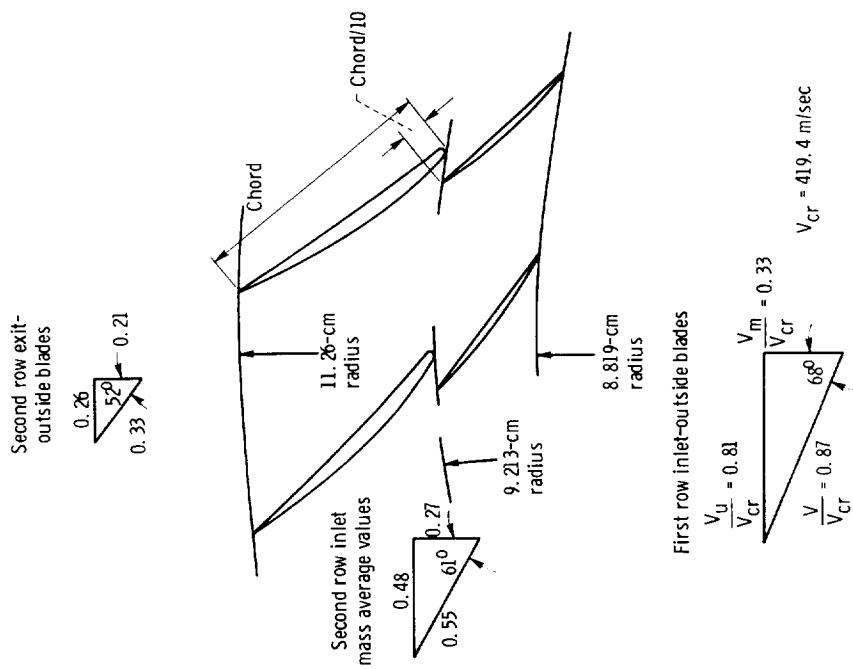
Figure 6. - Cascade vane arrangement and velocity diagrams.
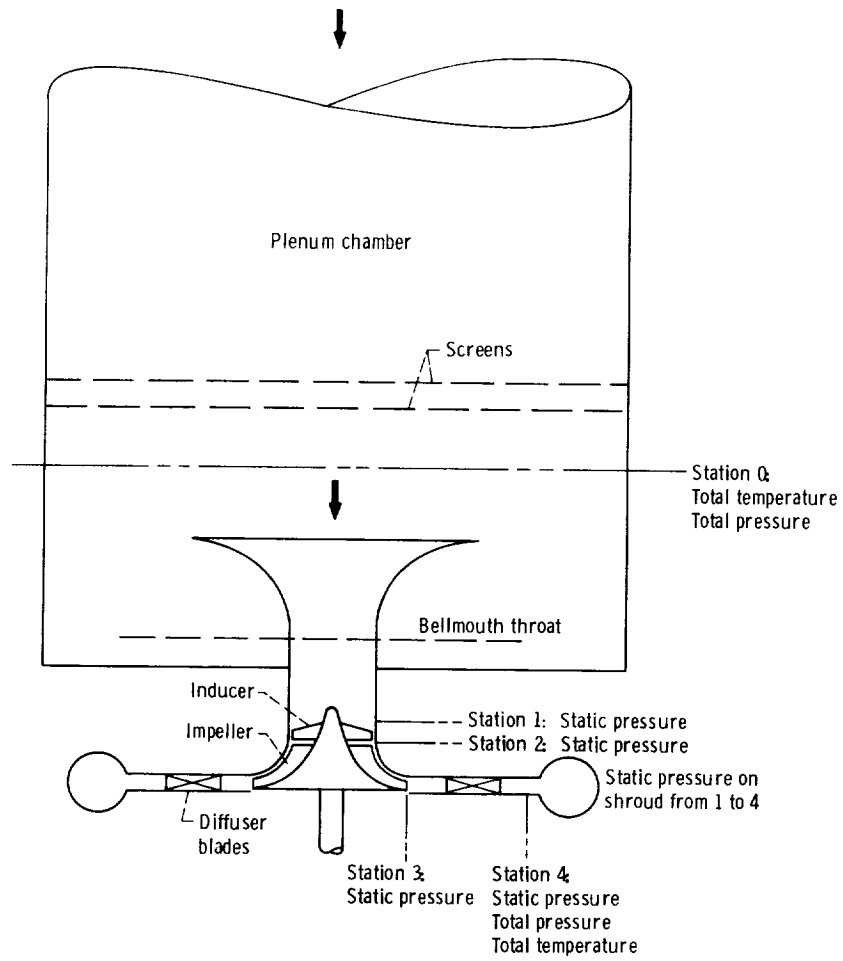
Figure 8. - Inlet, exit, and bellmouth measuring stations.

Plenum chamber

Screens

Station 0:
Total temperature
Total pressure

Bellmouth throat

Inducer
Impeller

Station 1: Static pressure
Station 2: Static pressure

Static pressure on
shroud from 1 to 4

Diffuser
blades

Station 3:
Static pressure

Station 4:
Static pressure
Total pressure
Total temperature
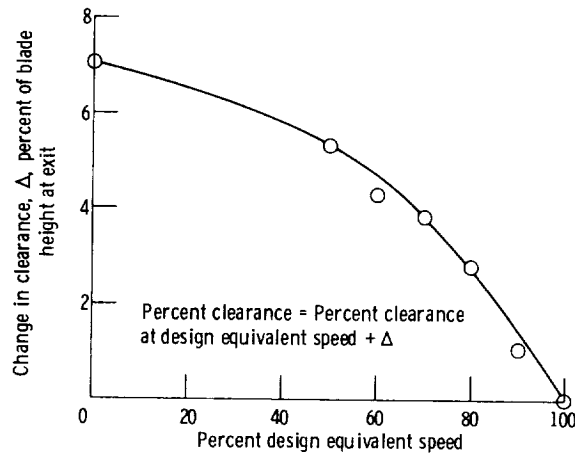
Figure 9. - Change in percent clearance as function of
equivalent speed.

Percent clearance = Percent clearance
at design equivalent speed + Δ

18
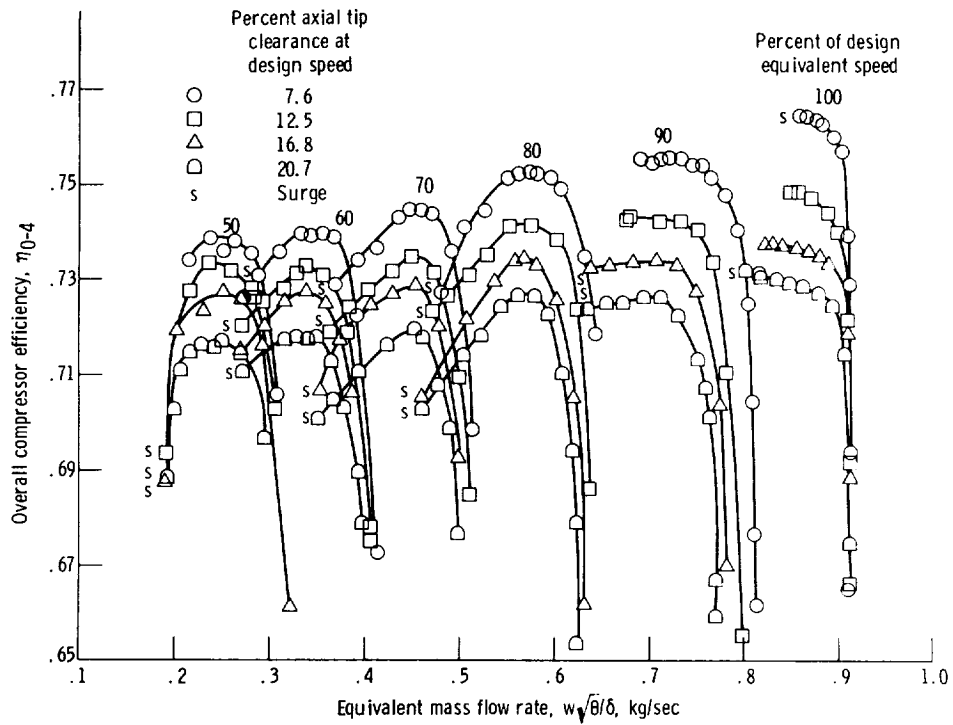
Figure 10. - Variation of total efficiency with equivalent mass flow, equivalent speed, and axial tip clearance. Cascade diffuser test.
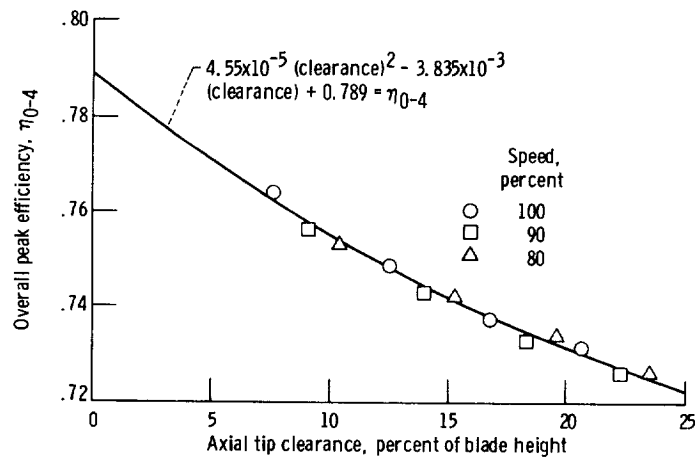
Figure 11. - Variation of peak efficiency with hot axial tip clearance. Cascade diffuser test.

19
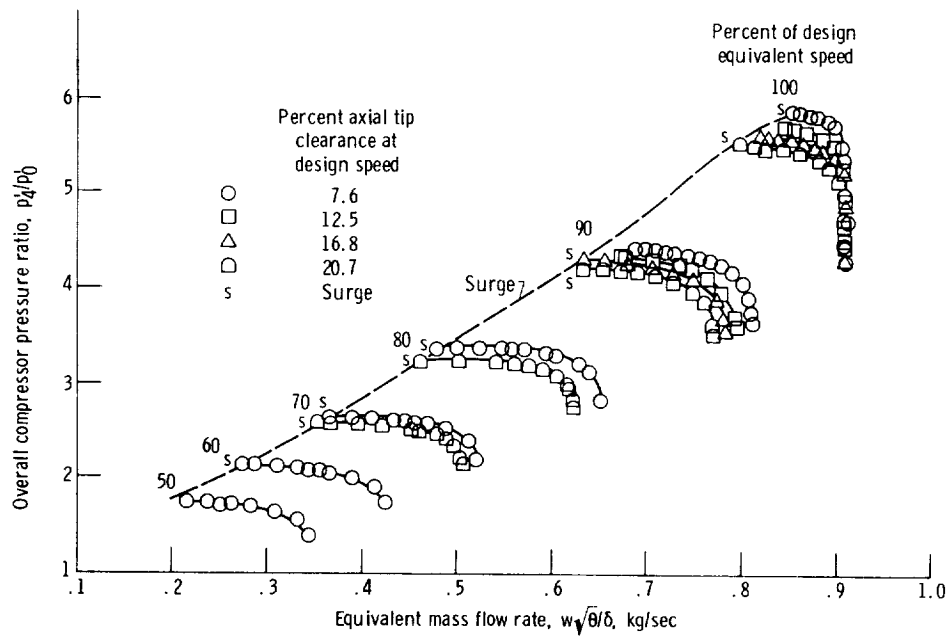
Figure 12. – Variation of total pressure ratio with equivalent mass flow, equivalent speed, and axial tip clearance. Cascade diffuser test.
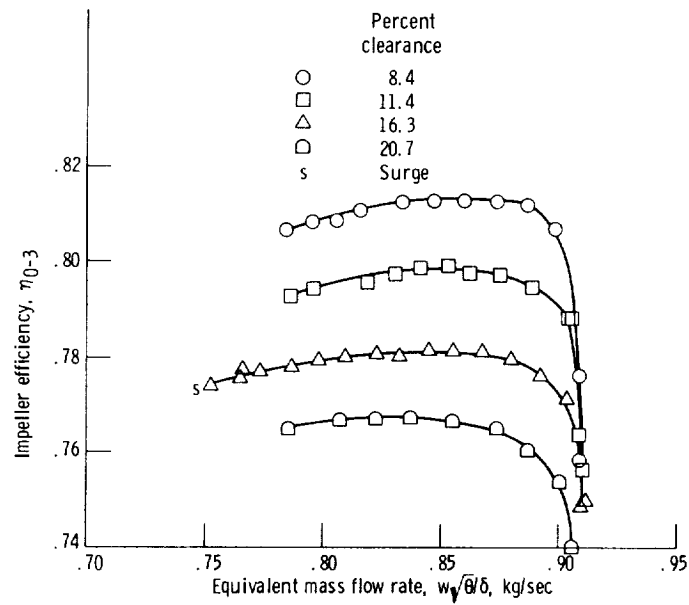
Figure 13. – Variation of impeller efficiency with flow rate and clearance at design speed. Vaneless diffuser test.

20
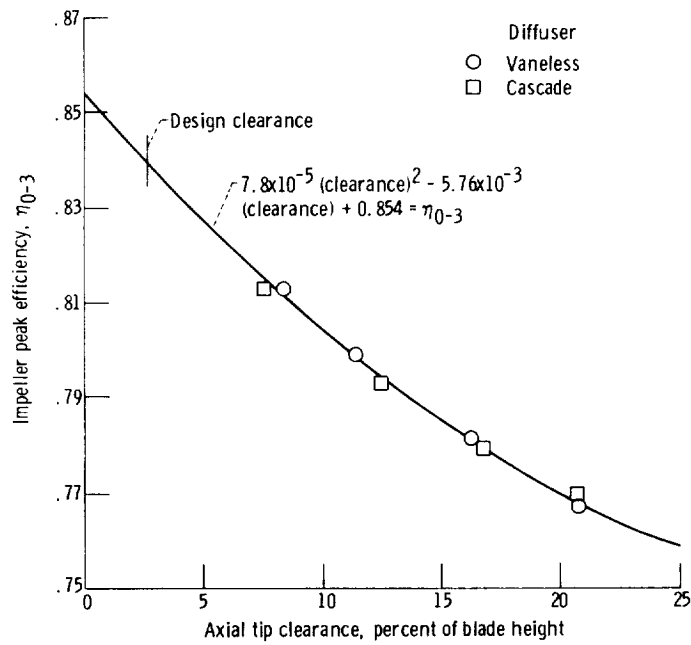
Figure 14. - Variation of impeller peak efficiency η_{0-3} with axial tip clearance at design speed.
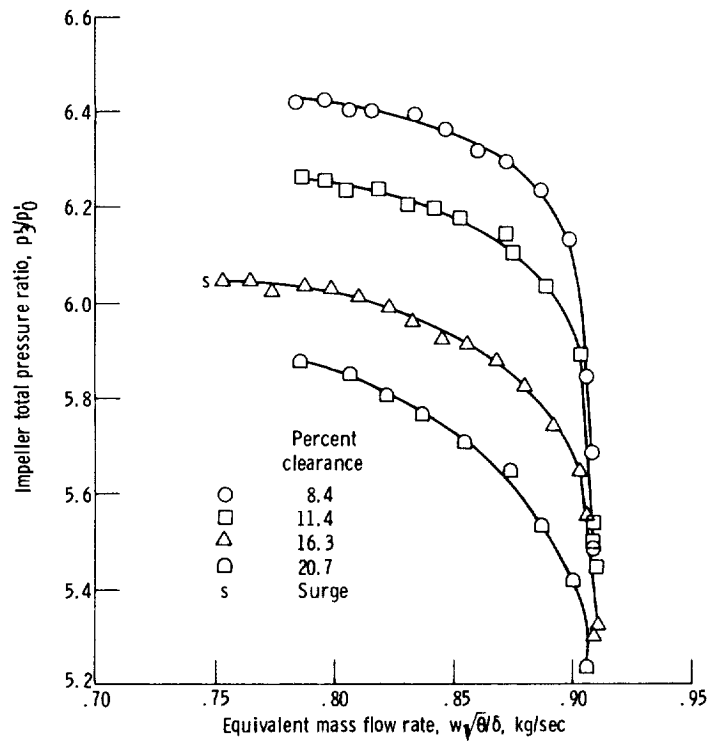
Figure 15. - Variation of impeller total pressure ratio with flow rate and clearance at design speed. Vaneless diffuser test.
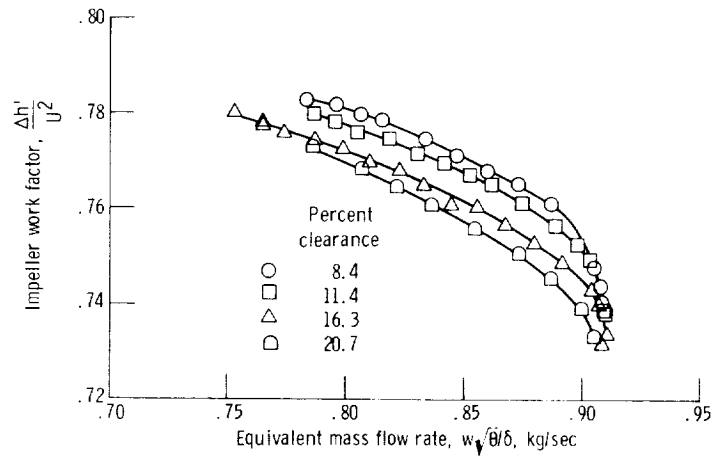
Figure 16. - Variation of impeller work factor with flow rate and clearance at design speed. Vaneless diffuser test.
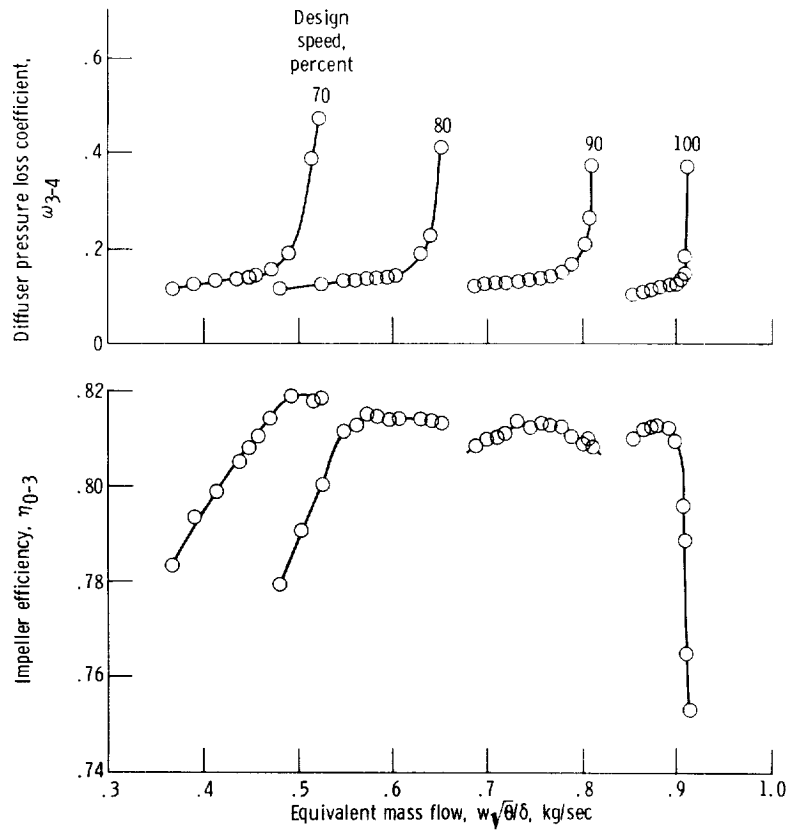

Figure 17. - Overall diffuser total pressure loss and impeller efficiency as function of mass flow. Cascade diffuser test; 7.6 percent clearance.
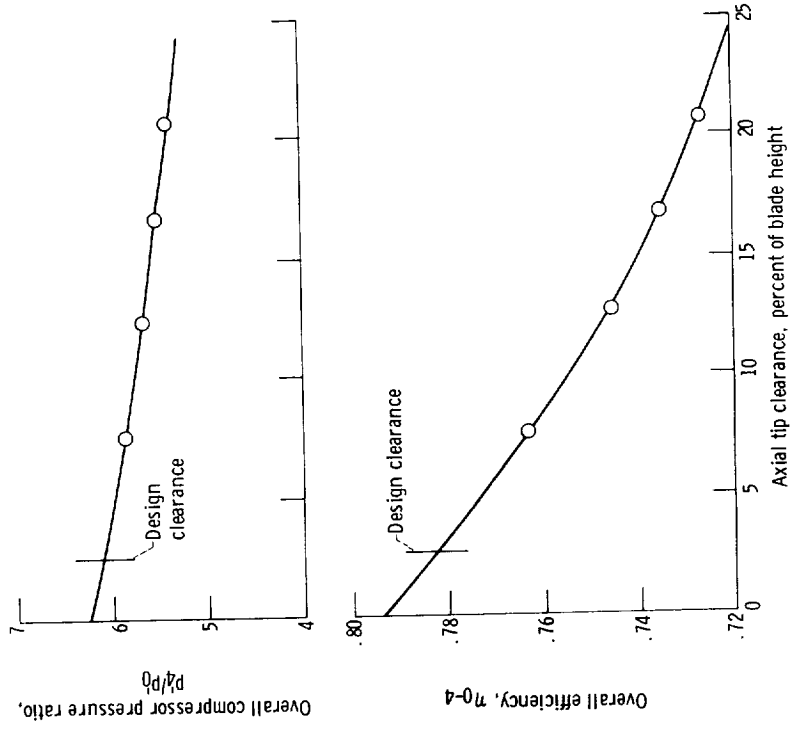
22

Figure 19. - Extrapolated stage performance at design clearance and design speed. Cascade diffuser test; mass flow rate, $w\sqrt{\theta}/\delta$, 0.878 kilogram per second.
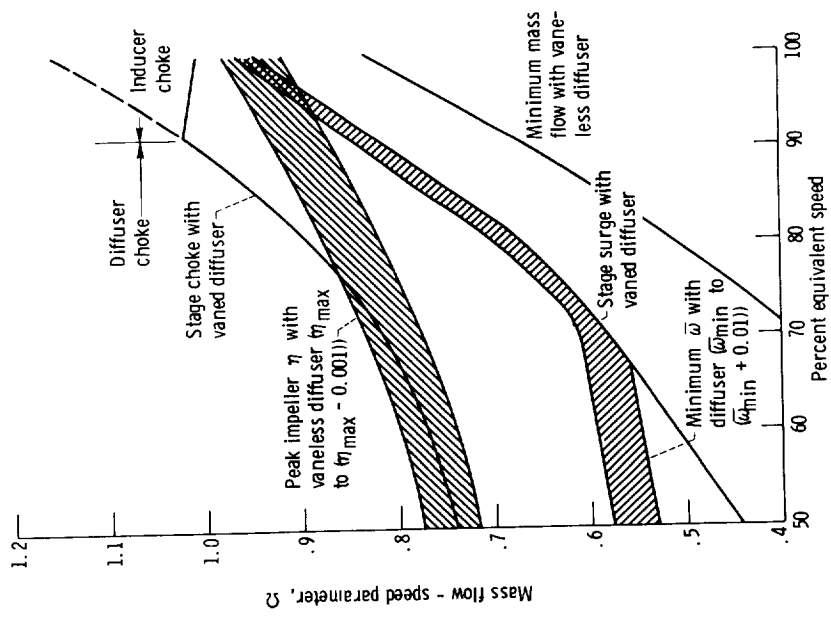

Figure 18. - Mass flow - speed parameter as function of percent equivalent speed showing relationship of impeller/ diffuser characteristics (vaned diffuser, 7.6 percent clearance, vaneless diffuser, 8.4 percent clearance).
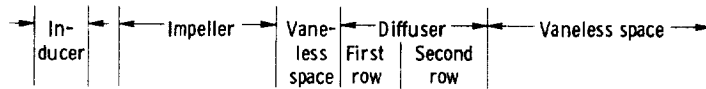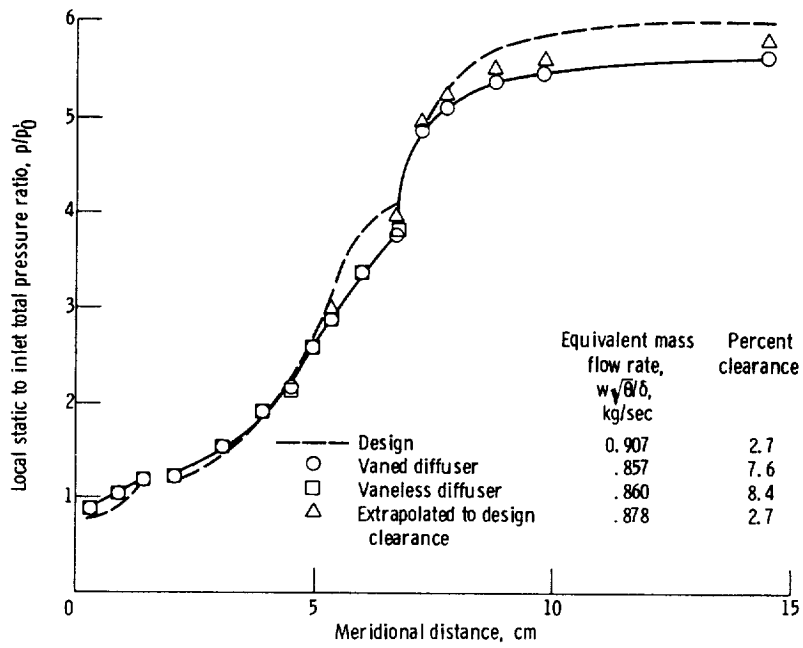
23

Figure 20. – Static pressure profiles for vaned to vaneless diffusers and extrapolated distribution at design clearance and design speed.

1. Report No. NASA TP-1091	2. Government Accession No.	3. Recipient's Catalog No.
4. Title and Subtitle EXPERIMENTAL PERFORMANCE OF A 13.65-CENTIMETER-TIP-DIAMETER TANDEM-BLADED SWEPTBACK CENTRIFUGAL COMPRESSOR DESIGNED FOR A PRESSURE RATIO OF 6		5. Report Date November 1977
		6. Performing Organization Code
7. Author(s) Hugh A. Klassen, Jerry R. Wood, and Lawrence F. Schumann		8. Performing Organization Report No. E-9206
9. Performing Organization Name and Address NASA Lewis Research Center and U.S. Army Air Mobility R&D Laboratory Cleveland, Ohio 44135		10. Work Unit No. 505-04
		11. Contract or Grant No.
12. Sponsoring Agency Name and Address National Aeronautics and Space Administration Washington, D.C. 20546		13. Type of Report and Period Covered Technical Paper
		14. Sponsoring Agency Code

15. Supplementary Notes

16. Abstract

A 13.65-cm-tip-diameter backswept centrifugal impeller having a tandem inducer and a design mass flow rate of 0.907 kg/sec was experimentally investigated to establish stage and impeller characteristics. Tests were conducted with both a cascade diffuser and a vaneless diffuser. A pressure ratio of 5.9 was obtained near surge for the smallest clearance tested. Flow range at design speed was 6.3 percent for the smallest clearance tested. Impeller exit to shroud axial clearance at design speed was varied to determine effect on stage and impeller performance.

17. Key Words (Suggested by Author(s)) Compressor Centrifugal compressor	18. Distribution Statement Unclassified - unlimited STAR Category 02	
19. Security Classif. (of this report) Unclassified	20. Security Classif. (of this page) Unclassified	21. No. of Pages 25	22. Price* A02